

Titles here

Accuracy of a portable Faraday cup for proton therapy beam current

Shaun Marshall (all G4 simulations)

Department of Physics, Worcester Polytechnic Institute, 100 Institute Rd, Worcester, MA 01609

Andrew D Hodgdon (all M6 simulations, leader of project)

Radsim, LLC, 584 Grove St, Newton, MA 02462 adhodgdon@radsim.org

Blake Currier (LATER)

Department of Physics, Worcester Polytechnic Institute, 100 Institute Rd, Worcester, MA 01609

LATER - Gordon or Boisseau for PFC construction and HIT measurements

LATER – B Gottschalk for providing insulator defect current model

LATER – Ethan Cascio if we do MGH experiments

LATER – abstract here

Purpose:

Methods:

Results:

Conclusions:

Key Words: Monte Carlo, Geant4, MCNP6, Faraday Cup, Proton Beam,

LATER - AUTHOR's PUNCH LIST

1. reformat the figure captions to be left and regular font, not titled.

1.0 INTRODUCTION

The Faraday cup is not now in the primary chain of clinical proton dosimetry which has been attributed to an 8 percent difference between FC and Air Kerma measurements [1]. However, the FC would be valuable for pencil beam dosimetry.

In modern radiation therapy, protons have become an increasingly popular method of treating cancer near critical structures, with many dosimetric advantages of charged particle interactions [1,2]. A novel, portable, vacuumless Faraday Cup for detecting charged particles was designed to calibrate proton therapy facilities, in energies ranging from 50 to 250 MeV. The detector is constructed of a copper cylinder, coated with Kapton insulation and grounded with silver (CITE). Monte Carlo computational simulations in MCNP6 (CITE) and GEANT4 (CITE) were performed to evaluate radiation cascade effects and predict signal versus height, diameter and insulator thickness characteristics.

Preliminary results indicated that increasing the mass of the Faraday Cup's conductor reduced proton leakage but increased the system accuracy. While additional Kapton captures more primary and secondary electrons, it also increases secondary electron leakage into the copper. Optimizing this Kapton thickness has been made difficult by the lack of low energy proton and electron cross-sections in current Monte Carlo based simulation programs (CITE). A comprehensive secondary electron evaluation of the Kapton was performed and benchmarked against a series of experimental measurements by J. Gordon et al [3].

Limited empirical evidence of proton-beam dose was available before the gold/aluminum-oxide Faraday Cup emulations at the Los Alamos National Laboratory, which produced charged-particle beam current yields as a function of (at the time, the highest) beam energies from 5-24 MeV; it was found that secondary electron yield varied inversely with impinging proton beam energy, fitting an inverse-root curve (as predicted by Sternglass) with approximately 10% error. [4,5]. This was later semi-empirically validated with similar models [6] and simulation using a constant-proportionality estimate of the secondary electron yield with the stopping power of protons in respective materials [7]; however, evidence exists which questions the validity of the latter approximation [8]. Though simulation techniques struggle to converge to comparable values for low beam energy scenarios, the findings establish a reasonable basis in setting the Faraday Cup depth to extend further than the material-specific range of the the particle. This removes the possibility of transmission-sputtering and second-surface electron emission occurrences, providing the user with a more controlled ammeter measurement [4].

LATER full narrative

2.0 METHODS AND MATERIALS

Define the defect. The percent charge defect is $100((I/B)-1)$. For example, if there are $2E9$ protons in the spill and PFC collected $1.98E9$, then the charge defect is -1% . I = PFC signal (current)

The defect associated with a particular charge detector can be measured when B for the beam is known.

2.1 PFC

LATER Full description of the design and construction of the PFC

The overall design was a pure copper cylinder, its axis on the beam.

LATER what about copper purity. three prototype Faraday Cup devices were constructed by Pyramid Technical Consultants, Inc. (Waltham, Ma), each with a different thickness of Kapton. The units were tested in Germany to determine accuracy of the new design.

A Portable Faraday Cup (PFC) is being designed to calibrate therapy-range proton accelerators (50 to 250 MeV). The PFC must be accurate to 1% and practical, hence vacuum-less and of low mass. Copper was chosen as the detector core, coated with a Kapton insulating film and silver ground. The Monte Carlo method (MCNP6 and Geant4) was used to simulate the radiation cascade and predict gain versus height (H), diameter (D) and insulator thickness (K). H and D were mostly functions of proton range; both are proportional to mass and inversely so to proton leakage, and thus decreases detector accuracy. Kapton functions to capture backscattered electrons, the function of the fields in a standard Faraday Cup. Greater K increases capture but increases secondary electron in-leakage. Determining optimal K was made difficult by the lack of low energy proton and electron cross-sections. A secondary electron model was programmed with the SDEF command for the MCNP model based on recently published cross-section approximations. This secondary electron source method was benchmarked against a series of experimental measurements of protons on copper.

2.2 HIT Measurements

LATER - Full description of the HIT measurements

Measured $D(K=59 \text{ to } 200\mu\text{m}, E=70 \text{ to } 221 \text{ | } H=10, R=6)$ where D = defect

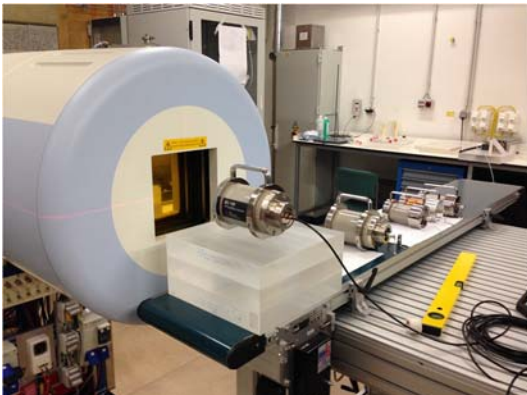
The defect, D , is

$$D = (E - 1) \cdot 100\%$$

$$E = \text{efficiency} = I/B$$

$$B = \text{proton charges in spill}$$

$$I = \text{signal (charges)}$$





2.3 MCNP6 Simulation

LATER describe mcnp6 version used, simulations of $D(H,R)$, decks in appendix,

LATER provide validation, i.e., comparisons of relevant experiments to MCNP

MCNP version 6.1 [2] with standard cross-section libraries was used to simulate signal in a solid copper cylinder with varying diameter and Kapton film thickness, and grounded with a layer of silver; the geometry is shown in Figure 2-1. The height of the cylinder is fixed at 10 cm, the diameter is varied from 2 to 10 cm and the Kapton thickness is varied from 25 to 75 microns. The materials are standard copper, Kapton, silver and air at STP. The source is a 2 cm diameter proton beam at 250 MeV. This is the maximum expected energy. A suitable diameter for this energy will be suitable for lower energies. Seven particles were tracked: neutrons, photons, electrons, protons, deuterons, tritons and alphas.

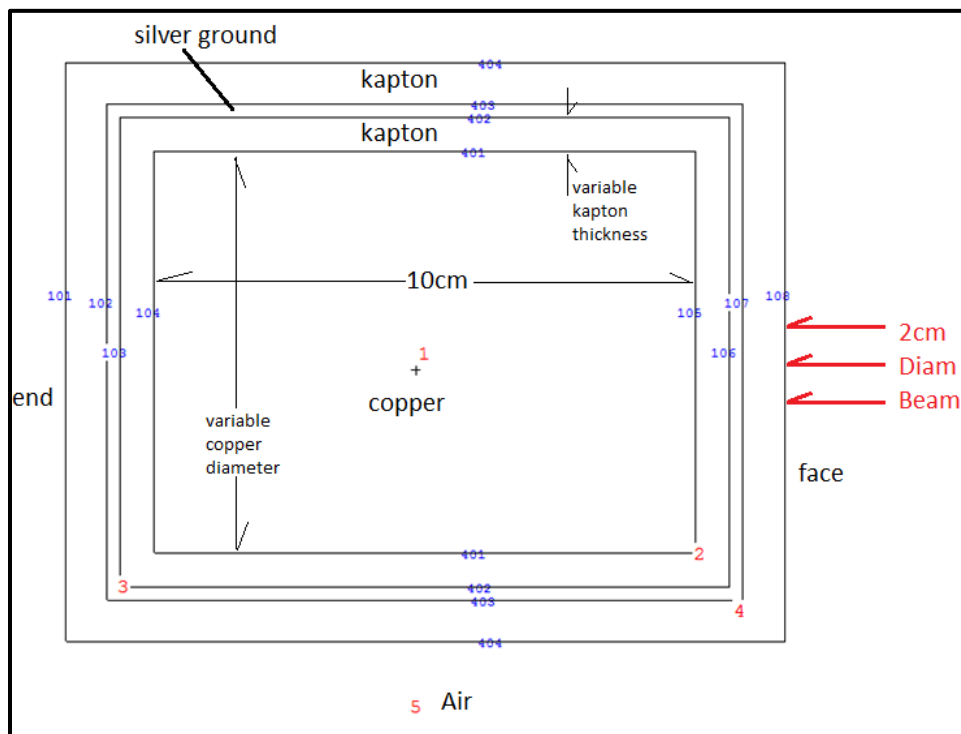


Figure 2-1: PFC Geometry in MCNP6 Model.

Signal, I_{MCNP} , was modeled as the sum of particles entering and leaving the copper.

$$I_{MCNP} = \sum(q_{in} - q_{out})/NPS$$

Where q is elemental charge, “in” and “out” indicates charge entering or exiting the copper through one of its three surfaces, front, side, end. And NPS is the number of particles started in MCNP’s “spill.”

Unfortunately, MCNP does not generate secondary electrons from proton collisions. It does generate electrons from gammas. It was assumed that the simulation of these secondary electrons was not required to determine the radius and length of the copper cylinder. This is reasonable given the very short range of even the most energetic expected electron. In this case the most energetic electron from the maximum energy proton is approximately $250 \text{ MeV}/1836 = 0.140 \text{ MeV}$ whose range in copper is about 50 μm .

- For the selection of a good copper diameter the SE_h are not important (untested)
- Protons and electrons are the only contributors to gain (valid within range of $2E-4$)
- The choice of copper diameter has little effect on the detailed behavior of SE_{th} electrons in Kapton (i.e., capture causing mirror charge in copper). This means that the location and energy of electrons captured in the kapton do not have to be tallied to get valid answer for the copper diameter (untested)

2.4 GEANT4 Simulation

LATER describe G4 simulation of $D(K=59 \text{ to } 200\mu\text{m}, E=70 \text{ to } 221 \text{ | } H=10, R=6)$ where $D = \text{defect}$

LATER describe hypothesis on how electrons thermalize (solvate) and turn to measureable current in an insulator between two conductors. Cite MLFC and BG correspondence

Table I summarizes the detector geometry of each run. The order of logical volume layers starting from the innermost are 1) the copper cylinder, 2) the Kapton1 film, 3) the silver paint layer, and 4) the Kapton2 film. Constructing cylindrical “layers” is as straightforward as defining a cylinder within another’s logical volume. Data were acquired as a function of impinging proton energy using the 50-250 MeV range as used in the HIT experiment. The Kapton1 thickness optimization was applied to this model both with and without the silver and secondary Kapton (+Ag/KA).

TABLE I. GEANT4 SIMULATION CYLINDRICAL CONSTRUCTION

Volume	Radius (mm)	Height (mm)
Copper	30	100
	Model	Thickness (μm)
Kapton1	S59	59
	S100	100
	S200	200
Silver	+Ag/KA	12
Kapton2	+Ag/KA	62

Geant4 is an object-oriented C++ toolkit for developing applications which simulate the passage of particles through matter. Libraries of cross-section tables, elemental/molecular properties, and pre-defined stochastic physics processes allow for rapid, intuitive invocation of necessary system setup commands. Once initialized, “Manager”

modules cooperate to organize and accumulate dynamic information of all affected particles. Each *event* (beam iteration) in a *run* (predefined geometry and physics for a series of events) stores the resulting *tracks* of particles which gained momentum, each for some number of *steps* where the defined physics governs the future pathway.

2.4.1 GEANT4 Model Setup

A useful feature of Geant4 is the ability to create user-defined actions (methods) throughout each module, which allows for a very fine-tuned analysis throughout the entire simulation. The following summarizes the custom details and methods for this application

- **DetectorConstruction.cc:** A copper cylinder of radius 3 cm and height 10 cm is covered in Kapton film of varying thicknesses: 59 μm , 100 μm and 200 μm . The film thickness is iterated by a function which is called before the command macro is examined. The top face of the copper lies in the $z = 0$ plane, with the beam approach the system from beneath.
- **SteppingAction.cc:** [For every step,] immediately checks if the step is the finale of a track. If so, the particle's vertex (original position) and destination volume and coordinates are found, and a charge signal calculation occurs. Entering/Leaving the copper gives a net signal of $\pm q$ where q is the charge of the particle. Entering/Leaving Kapton gives a relative proportionality of

$$s_{q,-KA} = \pm q \times \max[r\%, z\%], \quad (3)$$

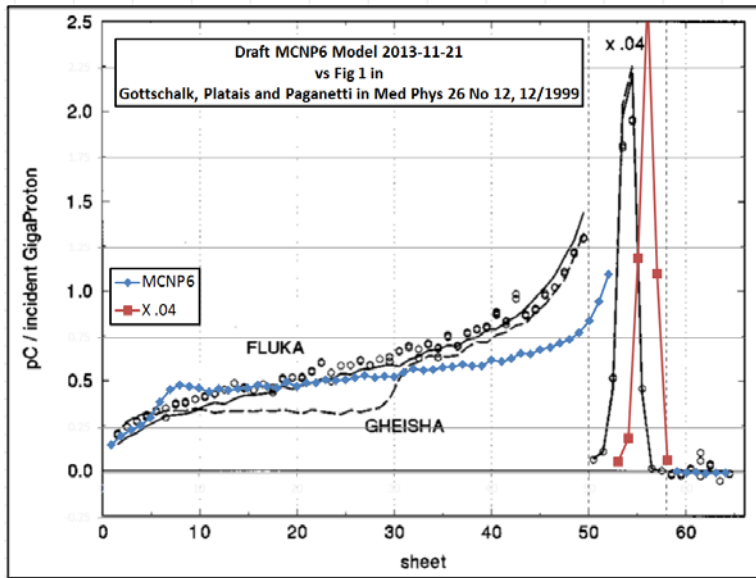
where $r\%$ is the percent distance away from the copper radially and $z\%$ is the percent distance away laterally. The signals are grouped and saved by a unique eventID number.

- **EventAction.cc:** At the end of each event, the signals are tallied, grouped, and saved by a unique runID number.
- **RunAction.cc:** At the end of each run, the average and standard deviation of the signals are acquired.

2.5 Methods Validation

A unique approach to the Faraday Cup, a series of copper sheets separated by Kapton insulators, was tested in the Harvard Cyclotron Laboratory at a much higher energy. This "Multilayer" prototype provided empirical data to benchmark the applicability of separate hadronic interaction modules of Geant3.2.1. Each sheet of Kapton offers a mid-range, low-interaction field within which secondary electrons (or other stray charged particles) and their abandoned ion may remain bound to each other [9]. This novel approach of "trapping" the electrons which would not otherwise be impeded by the dense metal localizes the effects of Coulombic scattering and normalizes the measured total signal of the charged particles scattered per unit length and beam input; a gain differential of depth, independent of contributions of secondary electrons in the air. The role of the vacuum to constrain particle flux was transferred to a silver external grounding brace in the experiments carried out by the Heidelberg Institute of Technology in a recent development to incorporate portability in measuring device. Current efforts are directed at establishing proof-of-concept theoretically with simulated reproduction.

The suitability of MCNP6 was benchmarked against two sets of experiments. The first was the multiplayer Faraday cup (BG99) and the second was electron backscatter secondary to protons by Borovsky et al[6].

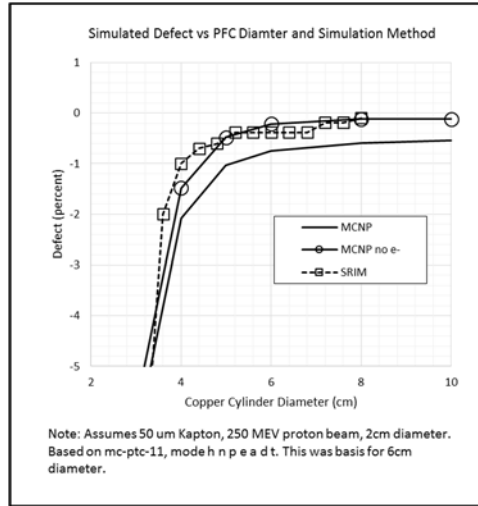


Overlaid on the figure from [3] is the prediction by MCNP6. *LATER - more*

3.0 RESULTS

3.1 Choice of PFC Radius

Fig. 2 shows the variation of error with copper diameter and method. Two methods are compared, SRIM (reference) and MCNP6. A conservative estimate of the error is found to drop below 1% beyond a 6 cm diameter. The same calculation was repeated with proton tallies alone, i.e., without any secondary electrons. This shows that if electrons had been completely ignored, the MCNP6 results would have been similar to the SRIM model and a diameter of 8 cm would have seemed reasonable.



3.2 Choice of Coating Thickness

Three pfc's, with different thickness of coating were made and simulated and tested.

3.3 Validation of Coating Thickness Model by Comparison to HIT Measurements

Measurements were made at HIT[4] and are shown in Table 3-1.

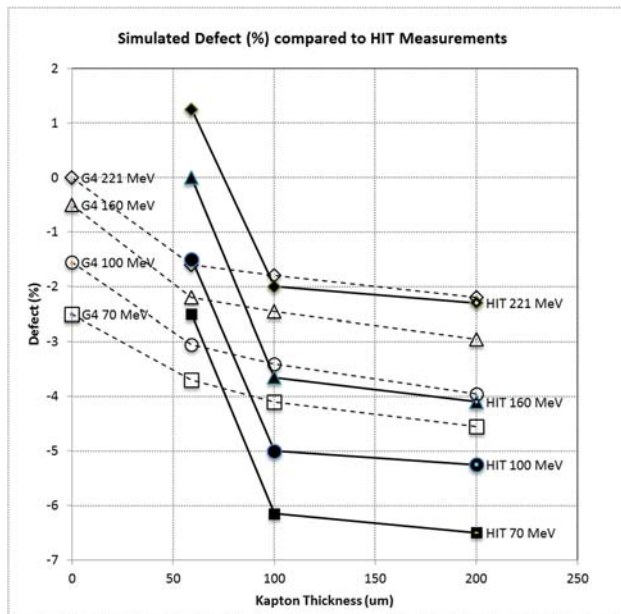
Table 3-1: Efficiency from HIT Experiment

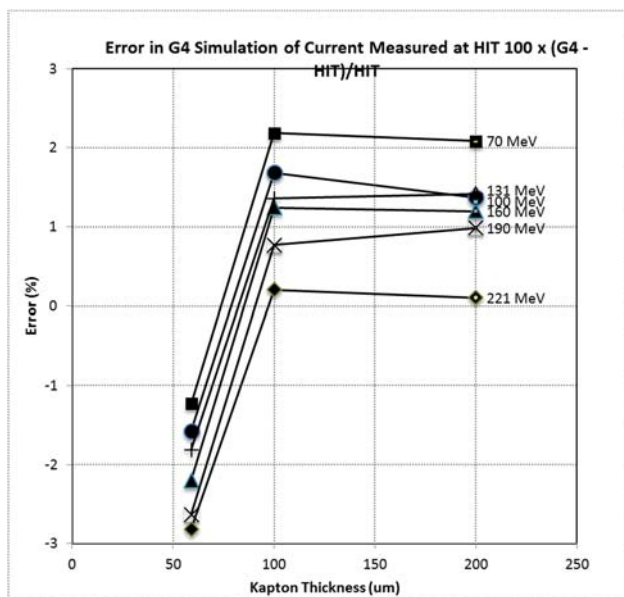
Energy (MeV)	S59	S100	S200
70.03	0.9750	0.9385	0.9350
100.46	0.9850	0.9500	0.9475
130.52	0.9925	0.9580	0.9525
160.09	1.0000	0.9635	0.9590
190.48	1.0075	0.9715	0.9650
221.06	1.0125	0.9800	0.9770

Charges entering and leaving the primary Kapton film covering the copper are subject to the linear proportion behavior defined in Eq. 3. Table IV shows a sample output of each model in both air and vacuum, the latter to remove oversaturation of beta emissions from the air due to delta-ray production (LATER: citation needed).

TABLE IV. PREDICTED EFFICIENCY FROM HIGH-ENERGY PROTONS USING GEANT4

Model	Energy (MeV)	(-Ag/KA)	(-Ag/KA) <i>in vacuo</i>	(+Ag/KA)	(+Ag/KA) <i>in vacuo</i>
S59	70.03	0.953588	0.974846	0.963133	0.963262
	100.46	0.967417	0.984694	0.970072	0.970867
	130.52	0.975593	0.990117	0.974286	0.976064
	160.09	0.981094	0.994044	0.978484	0.980236
	190.48	0.985111	0.996718	0.981775	0.983519
	221.06	0.988151	0.999012	0.984790	0.986344
	250.00	0.990298	1.000260	0.986376	0.987953
S100	70.03	0.953827	0.974725	0.962994	0.963440
	100.46	0.966795	0.984533	0.970114	0.970319
	130.52	0.975725	0.990464	0.974399	0.980993
	160.09	0.981055	0.994167	0.978401	0.976085
	190.48	0.985189	0.996801	0.981909	0.980045
	221.06	0.988149	0.999164	0.984451	0.983287
	250.00	0.990324	1.000160	0.986188	0.988118
S200	70.03	0.954372	0.974735	0.962984	0.963351
	100.46	0.966915	0.984373	0.970077	0.971036
	130.52	0.975377	0.990337	0.974646	0.976159
	160.09	0.980998	0.994016	0.978510	0.980092
	190.48	0.985217	0.996776	0.981840	0.983659
	221.06	0.988312	0.999045	0.984644	0.986081
	250.00	0.990213	0.999940	0.986601	0.988010





4.0 DISCUSSION

Why the is the C/M of the defect so large at low energies

What is the energy spectrum of the secondary n, g and e

What is the distribution of secondary n, g and e

What is utility of dose contours in the detector

Will the results of SEM (secondary emission monitors) tell us anything

Secondary vs tertiary electrons

4.1 Particle Cascade

The distribution of proton collisions from 50 beam protons is in Fig. 3. The distribution of 6 other particles (born of 50 Protons) is in Fig. 4; neutrons go everywhere. The distribution of electrons (just type SE_{lh}) is similar to photons. Table II shows the boundary crossings of neutral particles. In the problem there are about two neutral particle boundary crossings per beam proton. Table III shows the breakdown of gain from various charged particles for given directions and copper surfaces. This assumes 250 MeV Proton Beam, 6cm Copper Diameter and 50 microns kapton. The effect of secondary electrons produced directly by proton collisions (SD_h) is not included.

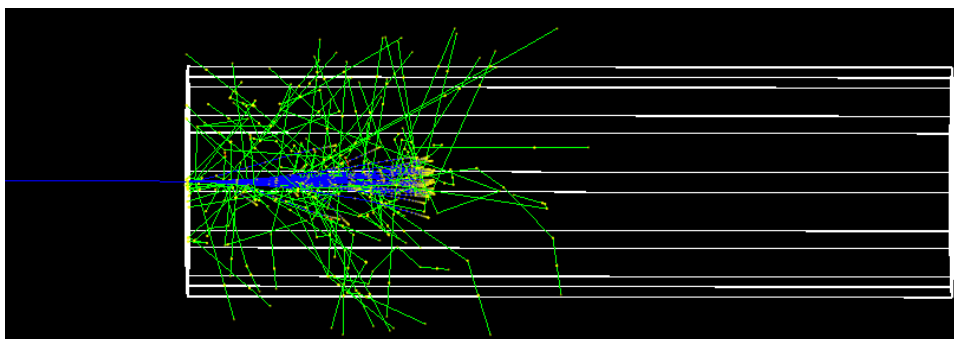
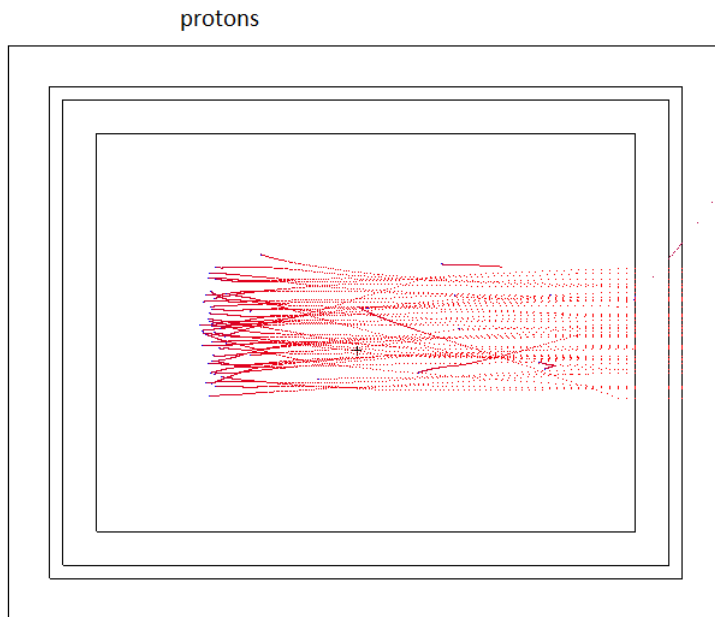


Figure 4-1: Particle Cascade from 250 MeV Protons impacting PFC as simulated by GEANT4. Fig. 5 depicts the tracks of particles given the simulation of 50 250 MeV protons entering the S59 model. The track color corresponds to particle charge, red for negative, blue for positive, and green neutral. As observed in the MCNP6 simulation, neutrons are scattered everywhere; for the most part, electrons created in the Faraday Cup do not travel far, as expected given their low-energy production and high stopping-power in copper.

1. **FIGURE 3. DISTRIBUTION OF 50 PROTONS OF ENERGY 250 MEV USING MCNP6. NOTE THE SINGULAR BACKSCATTER.**

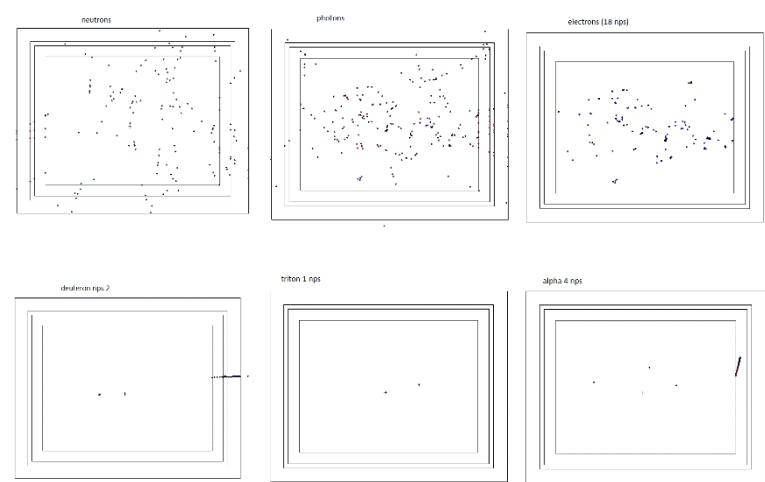


Figure 4. Distribution of six other particles

It is worth examining the behavior of the model. Kapton thickness (25, 50 and 75 microns) seems to make no difference in gain. Neither do the inclusion of tallies for deuterons, tritons and alphas, although the MCNP output file notes the absence of production cross-sections for these particles*. All of the figures and tables below were for the case of 6cm diameter, 50 microns of kapton and 50 beam protons of energy 250 MeV.

LATER – is following table correct?

TABLE II. CHARGES CROSSING COPPER SURFACES (FRACTION PER PROTON SOURCE) ASSUMING 250 MEV PROTON BEAM, 6 CM COPPER DIAMETER, 50 MICRONS OF KAPTON, AND NO SE_H

Particle	tally	face	cylinder	end	total
n	in	0.00065	0.00044	0.10692	0.10801
	out	0.14874	0.67867	0.00007	0.82747
γ	in	0.00038	0.00070	0.00011	0.00119
	out	0.17603	0.65051	0.07812	0.90466

Table III. Charges Crossing Copper Surfaces (fraction per proton source) assuming 250 MeV Proton Beam, 6 cm Copper diameter, 50 microns of Kapton, and no SE_h

Particle	tally	face	cylinder	end	total
P+	in	0.99997	0.00000	0.00000	0.99997
	out	0.00055	0.00123	0.00023	0.00201
	total	0.99941	0.00123	0.00023	0.99796
E (no SE _h)	in	0.00031	0.00087	0.00010	0.00128
	out	0.00149	0.00450	0.00051	0.00650
	total	0.00119	0.00362	0.00042	0.00523
d	in	0.00003	0.00000	0.00000	0.00003
	out	0.00007	0.00006	0.00002	0.00015
	total	0.00004	0.00006	0.00002	0.00012
t	in	0.00002	0.00000	0.00000	0.00002
	out	0.00003	0.00006	0.00002	0.00003
	total	0.00001	0.00006	0.00002	0.00001
a	in	0.00003	0.00000	0.00000	0.00003
	out	0.00003	0.00000	0.00000	0.00003
	total	0.00000	0.00000	0.00000	0.00000
Signal	in	0.99974	0.00087	0.00010	1.00124
	out	0.00082	0.00320	0.00026	0.00851
	total	0.99823	0.00485	0.00065	0.99273

4.2 Secondary Electrons

What is the impact of secondary electrons.

Three sources secondary electrons: delta rays (+ → - direct knock on, higher energy, max energy equation MeV/1836 etc), non delta rays, (what is the name, about 50% see ST57[5] , these are isotropic and low energy, so low, what does it matter.) and tertiary electrons, (my name, not from primary p+, but from n,p, n,g, g,3-) etc. Examine the energies of all cascade averaged over the copper.

Validation of the methods bo88. [6] shows that MCNP6 does not generate electrons secondary to protons. However, tertiary (my name) electrons from other interactions, like from gammas, are generated.

Therefore, there are delta rays and secondary electrons from protons that have not been accounted for. This means that the error is greater than has been portrayed and needs further investigation because it is shown in Fig. 2 that electron production (just the SE_{th}) is impacted by the diameter on the choice of diameter.

The electrons that are included are those that are secondary to the particle cascade subsequent to protons. For example, there are electrons secondary to photons that come from neutrons that come from protons. Table II shows that there are almost 2 neutral particles crossing the Faraday Cup boundary per beam proton. It is important to note that the addition of deuterons, tritons and alphas changes the gain by -0.0002[†], and that there were no proton creation cross-sections for Ag-107, so

it was substituted for Ag-109 which makes up about 2/3 of the silver.

[†] See mc-ptc-11-3.0-f for effect of deuterons, tritons, and alphas.

5.0 CONCLUSION

LATER – conclusion here

ACKNOWLEDGEMENTS

LATER – the following references need to be deleted or re-referenced from the text

- [1] W. Newhauser, N. Koch, S. Hummel, M. Ziegler, and U. Titt, “Monte Carlo simulations of a nozzle for the treatment of ocular tumours with high-energy proton beams,” *Physics in Medicine and Biology*, **50**, pp. 5229–5249 (2005).
- [2] J. M. Ryckman, “Using MCNPX to Calculate Primary and Secondary Dose in Proton Therapy,” *Georgia Institute of Technology* (2011), (Master’s thesis).
- [6] C. Castaneda, L. McGarry, C. Cahill, and T. Essert, “Secondary electron yields from the bombardment of Al₂O₃ by protons, deuterons, alpha-particles and positively charged hydrogen molecules at energies in the range of 10 to 80 MeV,” *Nuclear Instruments and Methods in Physics Research B*, **129**, pp. 199–202 (1997).
- [7] D. Kramer, “Design and Implementation of a Detector for High Flux Mixed Radiation Yields,” *Technical University of Liberec* (2008), (Doctoral dissertation).
- [8] A. Dubus et al., “Experimental and theoretical study of the ratio between the electron emission yield and the electronic stopping power for protons incident on thin carbon foils,” *Nuclear Instruments and Methods in Physics Research B*, **193**, pp. 621–625 (2002).

These references have been linked to the text

- 1. B. Gottschalk, 'A Poor Man's Faraday Cup,' Abstracts XIX PTCOG Meeting, Cambridge MA (1993) 13
- 2. MCNP6 Version 1.0 “MCNP6 User’s Manual,” Report la-cp-13-00634, May 2013.
- 3. B. Gottschalk, R. Platis, and H. Paganetti, “Nuclear interactions of 160 MeV protons stopping in copper: A test of Monte Carlo nuclear models,” *Medical Physics*, **26**, pp. 2597 (1999).
- 4. J. Gordon and L. Magallanes, “Evaluation of Current Measuring Beam Stop,” 2014, Proprietary Calculations.
- 5. E. Sternglass, “Theory of Secondary Electron Emission by High-Speed Ions,” *Physical Review*, 108, pp. 1 (1957).
- 6. J. E. Borovsky, D. J. McComas, and B. L. Barraclough, “The Secondary-Electron Yield Measured for 5-24 MeV Protons on Aluminum-Oxide and Gold Targets,” *Nuclear Instruments and Methods in Physics B*, **30**, pp. 191–195 (1988).